DAΦNE TECHNICAL NOTE

INFN - LNF, Accelerator Division

Frascati, December 19, 1994

Note: **L-20**

LOW BETA QUADRUPOLE FRINGING FIELD ON OFF-AXIS TRAJECTORY

C. Biscari

1. INTRODUCTION

DAΦNE, the Frascati Φ-factory[1], is a twin ring e^+ e^- collider. The target luminosity ($\mathcal{L} = 5 \times 10^{32}$ cm^{-2}s^{-1}) will be achieved with a maximum number of 120 stored bunches, crossing at an horizontal half angle of 12.5 mrad.

The two rings share two 10 m long Interaction Regions (IRs), where the opposite beams travel off-axis and cross at the Interaction Point (IP). Two experiments, KLOE[2] and FI.NU.DA.[3],will be installed in each one of the IRs. For the collider commissioning a DAY-ONE IR design[4] without detectors is foreseen, which can be used also on one IR in case only one of the experiments is installed in the rings for a certain period.

The fringing field multipolar expansion can be deduced from the longitudinal behaviour of the IR quadrupole field gradients, and introduced in the IR optics description. The DAY-ONE IR has been used to make some preliminary considerations on the effect of these non-linearities on the beam optics of the ring.

2. QUADRUPOLE POTENTIAL

The analytical expressions of the magnetic field near the axis can be derived from the general expression of the multipolar magnetic potential[5,6,7]. Following for example Bassetti's formalism, the scalar magnetic multipolar potential of order m in cylindrical coordinates can be written as:

$$Pm(r,q,z) = \frac{rm \sin(mq)}{m!}\, Gm(r,z) \tag{2.1}$$

where defining

$$G_m(r,z) = \sum_{k=0}^{\infty} G_{m2k}(z)\, r^{2k} \tag{2.2}$$

the functions $G_{m2k}(z)$ satisfy the following recurrence relationship:

$$G_{m2k}(z) = (-1)^k \frac{m!}{4^k (m+k)!\, k!} \frac{\partial^{2k} G_{mo}}{\partial z^{2k}} \tag{2.3}$$

A potential not depending on z contains only the first term of the sum (2.2) for each multipole, while if there is dependence on z, as in the fringing region of the quadrupole, the quadrupolar potential becomes:

$$P_2(x,y,z) = xy\,[\, G_{20}(z) + G_{22}(z)\, r^2 + G_{24}(z)\, r^4 + \ldots \,] \tag{2.4}$$

The field components, dropping terms of order higher than third, are then:

$$B_x(x,y,z) = y\,[G_{20}(z) + (3x^2 + y^2)\, G_{22}(z)] \tag{2.5}$$

$$B_y(x,y,z) = x\,[G_{20}(z) + (x^2 + 3y^2)\, G_{22}(z)\,] \tag{2.6}$$

$$B_z(x,y,z) = xy\,\left[\, \frac{\partial G_{20}(z)}{\partial z} + (x^2 + y^2)\, \frac{\partial G_{22}(z)}{\partial z}\,\right] \tag{2.7}$$

where, according to (2.3)

$$G_{22}(z) = -\frac{1}{12}\frac{\partial^2 G_{20}(z)}{\partial z^2} \tag{2.8}$$

If there is no dependence on the longitudinal coordinate, these field components coincide with the usual linear description. The function G_{22} adds cubic terms; it differs from a pure octupole in the coefficients of the $x^n y^m$ terms, and it is usually called pseudo-octupole. It must be pointed out that the third component B_z is essential to satisfy Maxwell equations, up to the truncation order.

3. QUADRUPOLAR POTENTIAL ALONG THE DAY-ONE IR

The DAY-ONE low beta IR layout consists of two quadrupole triplets on each side of the IP[4], plus one quadrupole placed on the IP, which is used as a fourth parameter to increase the flexibility of the IR design. The five central quadrupoles are 30 cm long and their bore radius is 5 cm. The two outer ones have larger apertures (±10 cm) and are 40 cm long. The nominal half crossing angle is θ_{cross} = 12.5mrad; the optics is designed to be compatible with θ_{cross} from 10 to 15mrad. Figure 1 represents the beam central trajectory in half IR for the different crossing angles. The trajectory passes in the three first quadrupoles at less than 3 cm from the axis, while inside the outer quadrupole the distance from the axis increases up to 5.6 cm for θ_{cross} = 15 mrad.

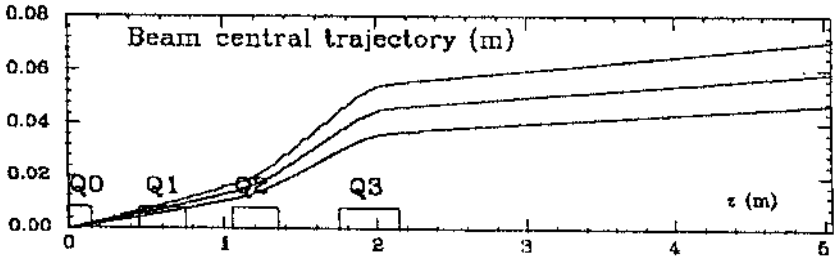

FIGURE 1. Beam Central Trajectory in half IR for θ_{cross} = 10, 12.5, 15 mrad.

Once determined the function G_{20}, all the field components are known for each quadrupole. Two methods have been used for this purpose.

First, the functions G_{20} and G_{22} have been deduced from the field measurements on the smaller quadrupole prototype[8]. Then the analytical formulae for the functions G_{nm} given in Bassetti's note[7] have been used; they are deduced from the expression of the potential created by a current distribution I_s on a cylindrical surface.

In particular, for a surface extending from $-z_L$ to z_L and radius R, the function G_{20} is:

$$G_{20}(z) = \frac{\mu_o I_s}{R^2} \left(\frac{9}{8} f_o(t) - f_1(t) + \frac{3}{8} f_2(t) \right) \Bigg|_{t_{min}}^{t_{max}} \tag{3.1}$$

with

$$f_k(t) = \left(\frac{t}{\sqrt{R^2 + t^2}} \right)^{2k+1} \qquad \frac{\partial f_k(t)}{\partial z} = -(2k+1)\frac{R^2}{t^3} f_{k+1}(t) \tag{3.2}$$

and $t_{max} = z_L - z$; $t_{min} = -z_L - z$. All the even(odd) derivatives of G_{20} can be written as linear combinations of $f_k(t)$ ($\frac{\partial f_k(t)}{\partial z}$).

The functions G_{20} evaluated with the two methods show a good agreement (see Fig. 2), so that in the following the analytical expressions will be used. They can also be used to describe the larger quadrupole. Figure 2a represents the G_{20} profile for the two quadrupole types. The analytically derived function G_{22} is plotted in Fig. 2b; to be noticed that for the same maximum gradient, the pseudo octupole function extends over a larger region for the larger radius quad, but its integrated strength is lower.

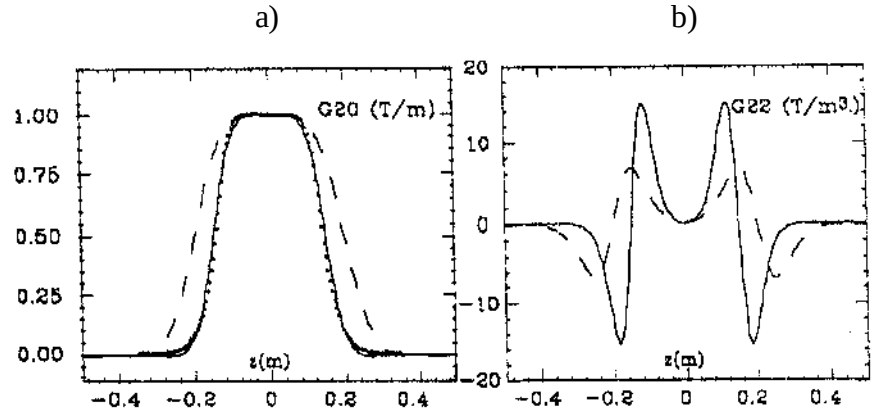

FIGURE 2. a) Analytical function $G_{20}(z)$ for the two quadrupole types (1: solid; 2: dashes), $G_{20}(z)$ as deduced from measurements for type 1 quadrupole (dots);
b) Analytical function $G_{22}(z)$ for the two quadrupole types (1: solid; 2: dashes).

4. FRINGING FIELD ON OFF-AXIS TRAJECTORY

The non linear fringing field effects are investigated by integrating the particle motion along the IR with the field components deduced from the function G_{20}. To explain the following results it is useful to expand the field components around the central trajectory Δx. The betatron oscillation is $x_\beta = x - \Delta x$, and defining:

$$A_0(z) = \Delta x\, G_{20}(z) + \Delta x^3\, G_{22}(z)$$
$$A_1(z) = G_{20}(z) + 3\,\Delta x^2\, G_{22}(z)$$
$$A_2(z) = 3\,\Delta x\, G_{22}(z)$$
$$A_3(z) = G_{22}(z)$$

the field components are:

$$B_x = A_1(z)\, y + A_3(z)\, y^3 + 3\,(2\,\Delta x + x_\beta)\, G_{22}(z)\, x_\beta y \tag{4.1}$$

$$B_y = \sum_{n=0}^{3} A_n(z)\, x_\beta^n + A_2(z)\, y^2 + 3\, x_\beta y^2\, G_{22}(z) \tag{4.2}$$

$$B_z = A'_0(z)\, y + A'_2(z)\, y^3/3 + [G'_{20}(z) + (3\Delta x^2 + r^2) G'_{22}(z)]\, x_\beta y + 3\Delta x\, G'_{22}(z)\, x_\beta^2\, y \tag{4.3}$$

(where $r^2 = x_\beta^2 + y^2$, and the primes indicate differentiation with respect to z of the functions G_{nm} and not of Δx). The functions $A_n(z)$ describe the part of the field depending on only one of the coordinates.

The 4x4 linear jacobian around Δx in half IR has been computed. Since the coupling is determined by non-linear terms the jacobian results uncoupled. The linear optics and therefore the optical functions depend on θ_{cross}, because the quadrupole gradients around the off-axis trajectory are described by the function $A_1(z)$. The resulting phase advance change is plotted in Fig. 3, adding the contribution of both IRs. It is larger in the vertical plane, because of the strong vertical IR focusing.

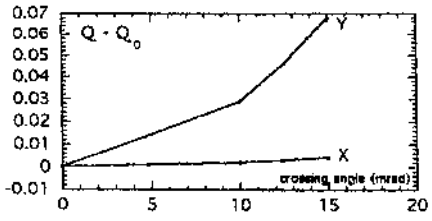

FIGURE 3. Difference between the phase advance off-axis and the phase advance on axis adding the contribution of the two IRs.

Multiturn tracking has been performed by integrating the particle motion along the IR and applying the linear matrix from the IR end to its beginning, matched to the values obtained from the jacobian computation. The IP has been set as the observation point of the phase plane. Other non-linearities of the lattice are not taken into account.

In the horizontal plane a slight phase advance increase with the amplitude (see

Fig. 4) appears. It becomes significant only after 10 σ_x, which is the nominal limit of the ring aperture. It is almost constant with the crossing angle. In fact the cubic term $A_{3(z)}$, main responsible for the tune shift with amplitude, does not depend on θ_{cross}. The total tune shift can be computed by including the effect of the fringing fields of all the ring quadrupoles.

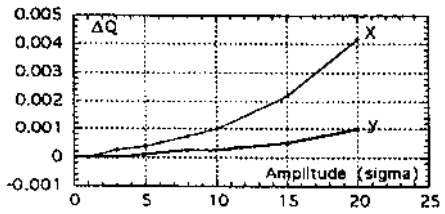

FIGURE 4. Horizontal and vertical phase advance increase versus amplitude for nominal tunes due to one IR contribution.

The motion in the vertical plane, for initial $x_\beta=x'_\beta=0$, transfers some momentum to the horizontal plane; the induced horizontal oscillation amplitude is proportional to the square of the vertical amplitude, and to θ_{cross} (see Fig. 5). It is bounded, and for the nominal coupling factor (κ = 0.01) negligible with respect to the natural beam horizontal dimensions. Figure 5b as an example represents the horizontal phase plane of a particle with initial coordinates $x_\beta=x'_\beta=y'=0$, $y=10\sigma_y$ (at κ = 0.01) and θ_{cross} = 12.5 mrad. The vertical phase advance increase with the amplitude, which, as expected, does not depend on θ_{cross}, is plotted in Fig. 4.

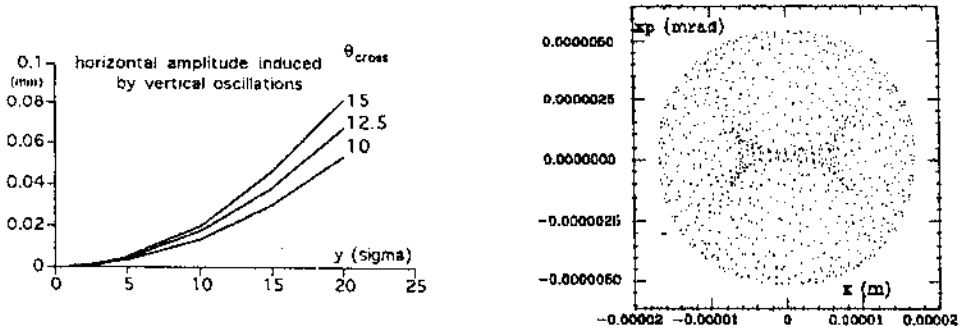

FIGURE 5. a) Induced horizontal oscillation amplitude as a function of vertical amplitude for the three different crossing angles, at the nominal tunes and nominal coupling factor.
b) Horizontal phase space of a particle with initial coordinate
$s\ x_\beta=x'_\beta=y'=0,\ y=10\sigma_y$ and θ_{cross} = 12.5 mrad.

Tracking particles with non negligible amplitude oscillations in both transverse planes results in a distortion of the transverse phase planes. It is negligible in the horizontal one, while an enlargening of the vertical ellipse appears, which increases with the horizontal amplitude and with the crossing angle. The effect is essentially due to the longitudinal component of the magnetic field, in particular to the last term in expression (4.3), which, being proportional to the square of x_β, does not average to zero on one horizontal oscillation. It means that a particle with any vertical amplitude when passing on the edges of the horizontal distribution will get an increase of its vertical invariant. If the vertical dimensions were comparable to the horizontal ones, for example for a non-flat beam, also the horizontal plane would be perturbed.

The vertical invariant with the nominal Twiss parameters at the IP ($W_y = y^2/\beta_y + \beta_y y'^2$) is shown in Fig. 6 as a function of the number of revolutions for a particle with 1,5,10 σ_x and 1 σ_y, together with the corresponding vertical phase space for the nominal tune values (5.18, 6.15) and nominal crossing angle.

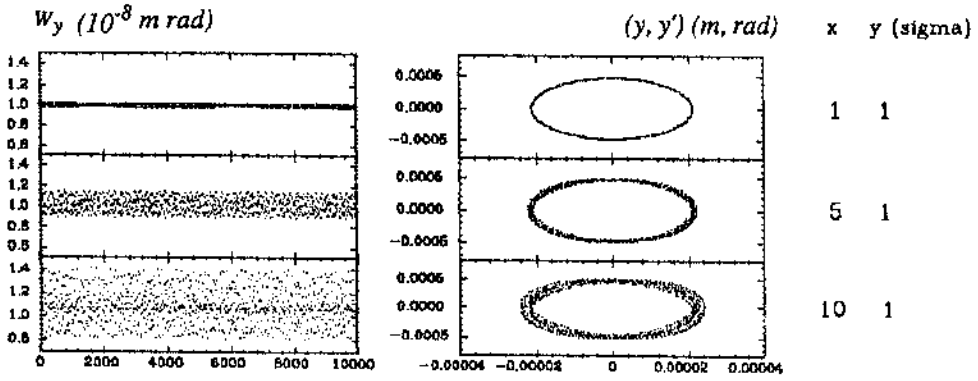

FIGURE 6. Vertical invariant versus turns (normalized to the vertical emittance at the nominal coupling $\varepsilon_y = 1\ 10^{-8}$ m rad) for a particle starting with $y = \sigma_y$, y' = 0. and x =1 (top), 5 (center) 10 (bottom) σ_x for the nominal tunes. Corresponding vertical phase space.

The relative variation of W_y at different vertical amplitudes is constant for the same horizontal amplitude. As in any coupling effects the magnitude of the distortion depends on the machine tune, and for the nominal tunes is not harmful. The relative variation of $\langle W_y \rangle$, where the average is taken over 1000 turns, is shown in Fig. 7, for some of the foreseen DAϕNE working points.

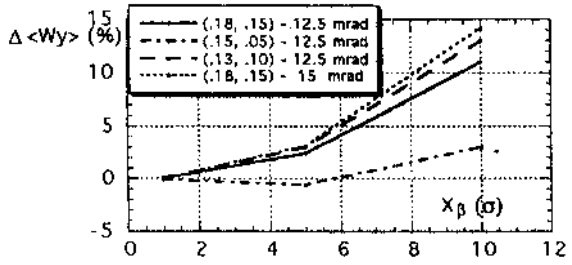

FIGURE 7. Variation in percentage of W_y in the most significant cases.

CONCLUSIONS

The fringing fields in the low-beta quadrupoles is not dangerous for DAϕNE operation. It produces different effects: one is a modification of the linear optics, which can be easily computed and matched to the ring arc optics. There is also an effect of non linear coupling of the transverse planes, which for some tune values can produce a vertical emittance increase for particles in the horizontal distribution tails. In the considered cases this increase is not dangerous (a maximum of 15% on the vertical invariant). Anyway, if necessary, it can be corrected by shifting the machine tune. Finally there is the well known tune shift on the amplitude, which is due to the pseudo-octupolar function and not to the off-axis trajectory, and which is present in all the ring quadrupoles.

ACKNOWLEDGMENTS

I thank M. Bassetti and M. Preger for many fruitful discussions.

REFERENCES

1. The DAΦNE Project Team, 'DAΦNE, The Frascati Φ-Factory', Proceeding of 1993 PAC, Washington, p.1993.

2. The KLOE collaboration - LNF-92/019(IR), April 1992.

3. The FI.NU.DA. Collaboration, LNF-93/021(IR), May 1993.

4. C. Biscari, 'Optimization of the DAY-ONE Interaction Region', DAΦNE Technical Note L-17, 1994.

5. S. Caspi, M. Helm, J.L. Laslett, '3D Field Harmonics', LBL-30313, March 1991.

6. S. Caspi, M. Helm, J.L. Laslett, 'The use of Harmonics in 3-D Magnetic Fields', IEEE Transactions on MAGNETICS vol. 30, n.4, p.2419, July 1994.

7. M. Bassetti, 'Analytical formulae for multipolar potentials', DAΦNE Technical Note G-26, 1994.

8. B. Bolli et al., DAΦNE Technical Note MM-4, 1994.